

Electronic structure of a mesoscopic superconducting disk: Quasiparticle tunneling between the giant vortex core and the disk edge

A. V. Samokhvalov,^{1,2} I. A. Shereshevskii,^{1,2} N. K. Vdovicheva,¹ M. Taupin,³
I. M. Khaymovich,^{4,1} J. P. Pekola,⁵ and A. S. Mel'nikov^{1,2}

¹*Institute for Physics of Microstructures, Russian Academy of Sciences, 603950 Nizhny Novgorod, GSP-105, Russia*

²*Lobachevsky State University of Nizhni Novgorod, 23 Prospekt Gagarina, 603950 Nizhni Novgorod, Russia*

³*Institute of Solid State Physics, Vienna University of Technology, Wiedner Hauptstrasse 8-10, 1040 Vienna, Austria*

⁴*Max Planck Institute for the Physics of Complex Systems, Nöthnitzer Strasse 38, 01187 Dresden, Germany*

⁵*QTF Centre of Excellence, Department of Applied Physics, Aalto University School of Science, P.O. Box 13500, 00076 Aalto, Finland*



(Received 4 January 2019; revised manuscript received 12 March 2019; published 15 April 2019)

The electronic structure of the giant vortex states in a mesoscopic superconducting disk is studied in a dirty limit using the Usadel approach. The local density of states profiles are shown to be strongly affected by the effect of quasiparticle (QP) tunneling between the states localized in the vortex core and the ones bound to the sample edge. Decreasing temperature leads to a crossover between the edge-dominated and core-dominated regimes in the magnetic field dependence of the tunneling conductance. This crossover is discussed in the context of the efficiency of quasiparticle cooling by the magnetic-field-induced QP traps in various mesoscopic superconducting devices.

DOI: [10.1103/PhysRevB.99.134512](https://doi.org/10.1103/PhysRevB.99.134512)

I. INTRODUCTION

Vortex states in mesoscopic superconducting (SC) systems of a size comparable to the superconducting coherence length have been well studied over the past few decades, mainly with the emphasis on the dependence of the vortex configuration on the size and geometry of the sample. In such nanoscale samples theory predicts that only a few vortices can be placed, and confinement effects result in different exotic vortex configurations unlike the triangular Abrikosov lattice [1–15]. These exotic configurations are formed by the interplay between imposed boundary conditions and the repulsive interactions between vortices.

The most remarkable consequence of this interplay is the formation of the so-called giant vortex state or multiquantum vortex when all the vortices merge in the disk center predicted mostly within the Ginzburg-Landau formalism provided the disk size is of the order of the coherence length. A variety of experimental methods have been used to verify these theoretical predictions: (i) Hall probe microscopy [4,6,16,17], (ii) Bitter decoration [18], (iii) scanning SQUID microscopy [19], and (iv) different tunneling experiments including scanning tunneling microscopy/spectroscopy studies [20–24].

The latter experimental approach is known to be sensitive to the electronic structure of the vortex states [25,26], namely, to the local density of states of quasiparticle excitations, and thus, the phenomenological Ginzburg-Landau theory often appears to be insufficient for the interpretation of the experimental data. This clear demand to the microscopic theory has stimulated theoretical activity in the field concentrated mainly on the calculations based on the Bogoliubov–de Gennes theory [12,13,27–37], i.e., on the clean limit corresponding to the very large mean-free path ℓ well exceeding both the coherence length ξ_0 and the sample size. Certainly, the predictions made

within such approach may be difficult to use for most of the experimentally available samples for which the dirty limit conditions ($\ell \ll \xi_0$) are much more appropriate. In particular, it is natural to expect that all the density of states features associated, e.g., with the different anomalous spectral branches [38] in the giant vortex or with the mesoscopic oscillations of the Caroli–de Gennes–Matricon energy levels [34] due to the finite sample size should be smeared by disorder. An adequate theoretical description of the sample electronic structure in this diffusive regime should be, of course, based on the Usadel-type theory. And indeed such calculations are known to provide an excellent tool for the analysis of the Abrikosov vortex lattices in unrestricted geometries (see, e.g., [39,40]). For multiquantum giant vortices these results have been generalized in Ref. [41] without accounting for the effect of the sample boundary.

It is important to note that the demand in the theoretical explanation of the available data of scanning tunneling microscopy and spectroscopy (STM/STS) on the exotic vortex structures in mesoscopic samples (see, e.g., [42,43]) is not the only motivation for the continuing research work in the field. Nowadays, superconducting nanostructures have become an important element in designing devices for rapidly expanding fields of quantum computing, quantum memory, superconducting logic, and metrology, and they are obviously the main building blocks for the superconducting electronics. However, superconductors are known to be easily poisoned by nonequilibrium quasiparticles, and these extra excitations drastically affect the performance of the above-mentioned quantum devices, e.g., via overheating or unwanted population in general. To suppress overheating in a superconductor different types of quasiparticle traps are used (see, e.g., Refs. [44–46] and references therein). One of the possible

range. Focusing on the axisymmetric multiquantum vortex states with the vortex core positioned in the center of the disk $r = 0$,

$$\Delta(\mathbf{r}) = \Delta_L(r) e^{iL\varphi}, \quad (1)$$

we consider solutions homogeneous along the z axis and characterized by a certain angular momentum L , referred to further as vorticity,

$$\mathcal{F}(\mathbf{r}, \omega_n) = \mathcal{F}_L(r, \omega_n) e^{iL\varphi}. \quad (2)$$

Here we choose the cylindrical coordinate system (r, φ, z) and the gauge $\mathbf{A} = (0, A_\varphi, 0)$, $A_\varphi = rH/2$. Due to the symmetry of Usadel equations, \mathcal{F} is an even function of ω_n , $\mathcal{F}(r, -\omega_n) = \mathcal{F}(r, \omega_n)$, so that it is enough to treat only positive ω_n values. In the standard trigonometrical parametrization $\mathcal{G} = \cos \theta_L$, $\mathcal{F} = \sin \theta_L e^{iL\varphi}$, $\mathcal{F}^\dagger = \sin \theta_L e^{-iL\varphi}$, the Usadel equations take the form

$$-\frac{\hbar D}{2} \left[\frac{1}{r} \frac{d}{dr} \left(r \frac{d\theta_L}{dr} \right) - \left(\frac{L - \phi_r}{r} \right)^2 \sin \theta_L \cos \theta_L \right] + \omega_n \sin \theta_L = \Delta_L(r) \cos \theta_L. \quad (3)$$

The self-consistency equation for the singlet superconducting order parameter function reads

$$\frac{\Delta_L(r)}{g} - 2\pi T \sum_{n \geq 0} \sin \theta_L = 0. \quad (4)$$

Here $D = v_F l / 3$ is the diffusion coefficient, $\Phi_0 = \pi \hbar c / e$ is the flux quantum, $\omega_n = \pi T (2n + 1)$ is the Matsubara frequency at the temperature T , $\phi_r = \pi r^2 H / \Phi_0$ is a dimensionless flux of the external magnetic field \mathbf{H} threading the circle of certain radius r , and the pairing parameter g determines the bare critical temperature T_{cs} as

$$\frac{1}{g} = \sum_{n=0}^{\Omega_D / (2\pi T_{cs})} \frac{1}{n + 1/2} \simeq \ln[\Omega_D / 2\pi T_{cs}] + 2 \ln 2 + \gamma, \quad (5)$$

with the Debye frequency Ω_D and the Euler-Mascheroni constant $\gamma \simeq 0.5772$. The coherence length $\xi_0 = \sqrt{\hbar D / 2\Delta_0}$ plays the role of a typical length scale in the Usadel equations.

The equations (3), (4) should be supplemented with the boundary conditions at the disk edge $r = R$:

$$\left. \frac{d\Delta_L}{dr} \right|_R = \left. \frac{d\theta_L}{dr} \right|_R = 0. \quad (6)$$

III. CRITICAL TEMPERATURE OF SUPERCONDUCTING TRANSITIONS WITH DIFFERENT VORTICITIES

For the temperatures close to the critical temperature of the superconducting transition $T \lesssim T_c(H)$, we can restrict ourselves to the solution of the Usadel equations (3) and (4) linearized in the anomalous Green's function ($\sin \theta_L \simeq \theta_L$):

$$-\frac{\hbar D}{2} \left[\frac{1}{r} \frac{d}{dr} \left(r \frac{d\theta_L}{dr} \right) - \left(\frac{L - \phi_r}{r} \right)^2 \theta_L \right] + \omega_n \theta_L = \Delta_L(r), \quad (7)$$

$$\frac{\Delta_L(r)}{g} - 2\pi T \sum_{n \geq 0} \theta_L = 0. \quad (8)$$

In these linearized equations the relation between the anomalous Green's function $\theta_L(r)$ and the order parameter $\Delta_L(r)$ can be written in the standard form

$$\theta_L(r, \omega_n) = \frac{\Delta_L(r)}{\omega_n + \Omega_L}, \quad (9)$$

where Ω_L is the depairing parameter depending on the disk radius R and the external magnetic field \mathbf{H} . Thus, the solution of Eq. (7) in the region $r \leq R$ can be expressed via the confluent hypergeometric function of the first kind (Kummer's function $K(a, b, z)$) [60]:

$$\Delta_L(r) = \theta_L(r) (\omega_n + \Omega_L) = C_L f_L(\phi_r), \quad (10a)$$

$$f_L(\phi_r) = e^{-\phi_r/2} \phi_r^{L/2} K(a_L, b_L, \phi_r). \quad (10b)$$

Here C_L is a constant, and the parameters a_L and b_L depend on the vorticity L as follows (see Appendix for details):

$$a_L = \frac{1}{2} \left(|L| - L + 1 - \frac{\Phi_0 \Omega_L}{\pi \hbar D H} \right), \quad b_L = |L| + 1.$$

The boundary condition (6) for the orbital mode L written in the form (10) results in the following algebraic equation:

$$\Gamma_L(a_L, \phi) = b_L (|L| - \phi) K(a_L, b_L, \phi) + 2\phi a_L K(a_L + 1, b_L + 1, \phi) = 0. \quad (11)$$

Equation (11) determines the implicit dependence of the parameter a_L on the flux $\phi(H) = \pi R^2 H / \Phi_0 \equiv H / H_0$ through the disk for a fixed value of vorticity L normalized to the flux quantum. Here we introduced a characteristic field $H_0 = \Phi_0 / \pi R^2$.

The solutions $a_L^{(n)}$ of Eq. (11) give a set of values $\Omega_L^{(n)}$ that depend on the normalized flux threading the whole disk ϕ and the disk radius R : $\Omega_L = \Omega_L(\phi, R)$. Finally, substituting the expression (9) into the self-consistency condition (8) one obtains the following equation for the critical temperature T_L of the state with the vorticity L :

$$\ln \frac{T_L}{T_{cs}} = \Psi\left(\frac{1}{2}\right) - \Psi\left(\frac{1}{2} + \frac{\Omega_L}{2\pi T_L}\right), \quad (12)$$

where Ψ is the digamma function. In accordance with the self-consistency equation (12), the minimal value of the depairing parameter

$$\Omega_c = \min_{L, n} \{ \Omega_L^{(n)}(\phi, R) \} \quad (13)$$

determines the vorticity L_c and the critical temperature $T_c = T_{L_c}$ of the orbital mode, which nucleates in the disk of the radius R placed in the external magnetic field \mathbf{H} .

Figure 2 shows typical dependencies of the critical temperature T_c and the depairing parameter Ω_c on the external magnetic flux ϕ across the disk for a fixed value of the disk radius R . The phase boundary $T_c(\phi)$ exhibits an oscillatory behavior similar to the well-known Little-Parks oscillations [61,62], caused by the transitions between the states with different angular momenta L . The values of the normalized flux through the disk ϕ_L , where the switching of the orbital

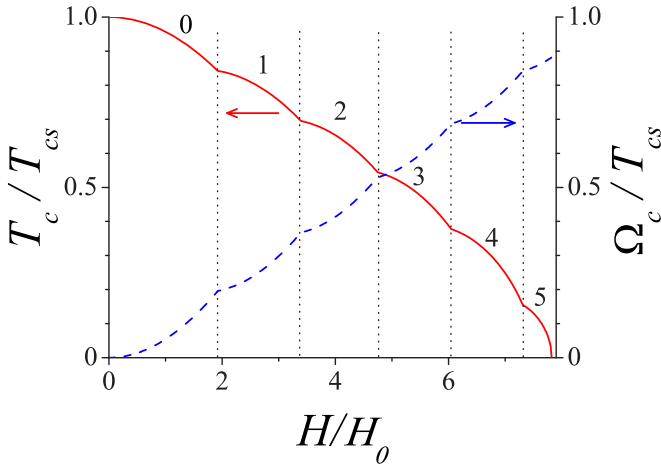


FIG. 2. The dependence of the critical temperature T_c (solid red line) and the depairing parameter Ω_c (dashed blue line) on the external magnetic field. Here we choose $R = 4\xi_0$. The numbers near the curves denote the corresponding values of the vorticity L_c . The dotted vertical lines correspond to the fluxes $\phi = \phi_L$, where the switching of the orbital modes $L \rightleftharpoons L + 1$ takes place.

modes $L \rightleftharpoons L + 1$ takes place, obey the equations

$$\Gamma_L(a_L, \phi_L) = 0, \quad \Gamma_{L+1}(a_{L+1}, \phi_L) = 0, \quad (14)$$

and do not depend on the disk radius R : $\phi_L \simeq 1.92, 3.40, 4.74, 6.04, 7.30, \dots$ for $L = 0-5 \dots$. The

magnetic field of the switching between modes L and $L + 1$ is determined by the expression $H_s = H_0\phi_L$. The values of the dimensionless fluxes corresponding to the vorticity switching coincide with the ones found in Ref. [10] for a superconducting disk within the Ginzburg-Landau theory. This coincidence comes from the obvious fact that the linearized Usadel equation (7) after the substitution of the expression (9) becomes similar to the linearized Ginzburg-Landau equation. Surely, this similarity does not extend to the full behavior of the $T_L(H)$ curve determined by Eq. (12). Note also that both the depairing factor and, thus, the critical temperature depend strongly on the disk radius R : $\Omega_L \sim R^{-2}\tilde{\Omega}_L(\phi)$, where $\tilde{\Omega}_L(\phi)$ is a certain function of the dimensionless flux ϕ only. One can see that the decrease in the R value results in the decrease in the number of observable different vortex states.

IV. DENSITY OF STATES

For a fixed temperature T the orbital mode L exists in the interval of the magnetic field values $0 \leq H_{L1} \leq H \leq H_{L2}$ that satisfy the condition $T_L(\phi(H)) \geq T$ (see the inset in Fig. 3). Figure 3 shows a typical temperature dependence of the upper critical field for the disk,

$$H_{c2} = \max_L \{H_L(T)\},$$

affected by the transitions between different orbital states. In order to analyze the characteristics of the sample far from the phase transition line we return back to the nonlinear Usadel theory and consider the full free energy functional:

$$F_L = 2\pi N_0 w \left(\pi T \sum_{\omega_n < \Omega_D} \int_0^R r dr \left\{ \hbar D \left[\left(\frac{\partial \theta_L}{\partial r} \right)^2 + \left(\frac{L - \phi_r}{r} \right)^2 \sin^2 \theta_L \right] - 4\omega_n \cos \theta_L - 4\Delta_L \sin \theta_L \right\} + \frac{1}{g} \int_0^R r dr \Delta_L^2 \right), \quad (15)$$

where N_0 is the density of states at the Fermi energy per one spin projection, and w is the disk thickness. Focusing now on the effect of the switching between different vortex states on the density of states we should note that experimentally this quantity can be most directly probed by the measurements of the local differential conductance:

$$G_L(V, r, \phi) = \frac{dI/dV}{(dI/dV)_N} = \int_{-\infty}^{\infty} d\varepsilon \frac{N_L(\varepsilon, r, \phi)}{N_0} \frac{\partial f(\varepsilon - eV)}{\partial V}, \quad (16)$$

where V is the applied bias voltage, $(dI/dV)_N$ is a conductance of the normal metal junction, and $f(\varepsilon) = 1/[1 + \exp(\varepsilon/T)]$ is the Fermi function.

A. High magnetic field: $H \lesssim H_{c2}$

We start our analysis from the limit of high magnetic fields close to the phase transition line $H_{c2}(T)$ shown in Fig. 3 when the solution of the Usadel equations can be significantly simplified due to the smallness of the functions Δ_L and θ_L . In this case one can use the solution of the linearized theory (9), (10). The constant C_L in Eq. (10a) should be found from the nonlinear Usadel theory (3). For this purpose we write the corresponding free energy up to the fourth power of Δ_L and θ_L :

$$F_L - F_N = 2\pi N_0 w \int_0^R r dr \left\{ \frac{\Delta_L^2}{g} - 2\pi T \times \sum_{\omega_n < \Omega_D} \left[\Delta_L \theta_L + \frac{\hbar D}{2} \left(\frac{L - \phi_r}{r} \right)^2 \frac{\theta_L^4}{3} + \omega_n \frac{\theta_L^4}{12} - \Delta_L \frac{\theta_L^3}{3} \right] \right\}, \quad (17)$$

where F_N is the free energy of the normal state. Using the above self-consistency equation for $T_c(H)$

$$\frac{1}{g} = \sum_{\omega_{nc} < \Omega_D} \frac{2\pi T_c(H)}{\omega_{nc} + \Omega_L} \quad (18)$$

with $\omega_{nc} = \pi T_c(H)(2n + 1)$, and the relation (9), we obtain

$$F_L - F_N \equiv -AC_L^2 + BC_L^4 = 4\pi^2 N_0 w \times \int_0^R r dr \left\{ \Delta_L^2 \left(\sum_{\omega_{nc} < \Omega_D} \frac{T_c(H)}{\omega_{nc} + \Omega_L} - \sum_{\omega_n < \Omega_D} \frac{T}{\omega_n + \Omega_L} \right) + \Delta_L^4 T \sum_{\omega_n < \Omega_D} \left[\frac{1}{4(\omega_n + \Omega_L)^3} + \frac{\Omega_L - 2\hbar D \left(\frac{L - \phi_r}{r} \right)^2}{12(\omega_n + \Omega_L)^4} \right] \right\}. \quad (19)$$

Here the first (second) line in r.h.s. corresponds to the quadratic (quartic) terms in $\Delta_L = C_L f_L(\phi_r)$.

Finally the amplitude C_L that minimizes the above functional $F_L = F_N - AC_L^2 + BC_L^4$ takes the form $C_L^2 = A/(2B)$, with

$$A = \frac{\Phi_0 N_0 w}{H} I_{2,0} \times [\Psi(\omega_{L,T_c}) - \Psi(\omega_{D,T_c}) - \Psi(\omega_{L,T}) + \Psi(\omega_{D,T})], \quad (20)$$

$$B = \frac{N_0 w}{6(2\pi T)^3} \left\{ \frac{\Phi_0 I_{4,0}}{2H} [6\pi T \zeta_3(\omega_{L,T}) + \Omega_L \zeta_4(\omega_{L,T})] - \pi \hbar D (I_{4,1} - 2LI_{4,0} + L^2 I_{4,-1}) \zeta_4(\omega_{L,T}) \right\}, \quad (21)$$

where $\zeta_k(a) = \sum_{n \geq 0} 1/(n+a)^k$ is the zeta function, $\omega_{L,T} = \Omega_L/(2\pi T) + 1/2$, $\omega_{D,T} = (\Omega_D + \Omega_L)/(2\pi T) + 3/2$, and

$$I_{n,k} = \int_0^\phi f_L^n(\phi_r) \phi_r^k d\phi_r. \quad (22)$$

Substituting now $\omega_n = -i\varepsilon$ in the relation (9), one obtains the following expressions for the LDOS valid to the first order

in $\Delta_L^2(r)$:

$$N_L(\varepsilon, r, \phi) = \text{Re}[\mathcal{G}(\varepsilon, r)] = \text{Re}[\cos \theta_L(r)]|_{\omega_n = -i\varepsilon} \approx 1 + \frac{\Delta_L^2(r)}{2} \frac{\varepsilon^2 - \Omega_L^2}{[\varepsilon^2 + \Omega_L^2]^2}. \quad (23)$$

The transitions between different vortex states while sweeping the magnetic field up are visualized by abrupt changes (or jumps) in ZBC [21,23,24], which are determined by the LDOS $N(\varepsilon, r, \phi)$ at the Fermi level $\varepsilon = 0$. Let us consider a certain point ($T = T_s$, $H = H_s$) at the phase diagram Fig. 3, where switching of the orbital modes $L \rightleftharpoons L + 1$ takes place, $H_s = H_0 \phi_L$. Since the depairing parameters of the orbital modes L and $L + 1$ coincide $\Omega_L = \Omega_{L+1}$ the corresponding jump in the LDOS $N_{L+1} - N_L$ at the disk edge $r = R$ can be estimated as follows:

$$N_{L+1} - N_L \Big|_{\substack{\varepsilon=0 \\ r=R \\ \phi=\phi_L}} \sim \frac{\Delta_L^2(R) - \Delta_{L+1}^2(R)}{2\Omega_L^2}. \quad (24)$$

Figure 4 shows the magnetic field dependence of the normalized LDOS at the disk edge. The transitions between different vortex states ($L \rightarrow L + 1$) are accompanied by the abrupt reduction in LDOS at the disk edge while sweeping the magnetic field up. Similar jumps of the LDOS, which are attributed to the entrance of a vortex inside the disk, have been observed in measurements of the normalized ZBC on Pb nanoislands [21] and MoGe nanostructures [24].

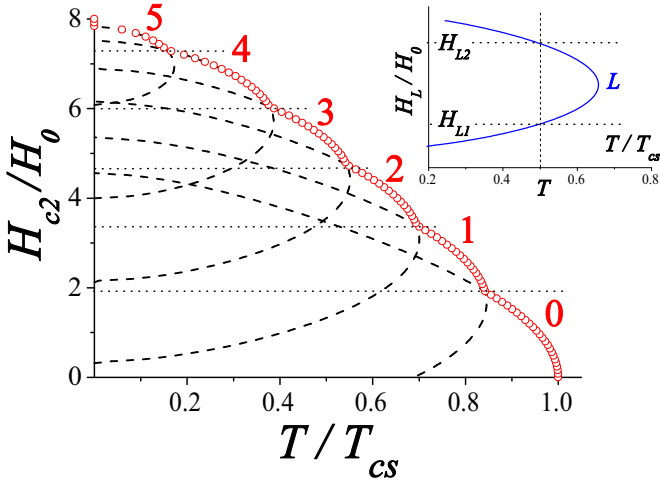


FIG. 3. Schematic temperature dependence of the upper critical field H_{c2} of superconducting phase transition of 2D disks (shown by red \circ). Dashed lines show the dependence of the critical magnetic fields $H_L(T)$ for the orbital mode with the vorticity L explicitly written in the plot. The dotted horizontal lines are given by the relation $\phi(H) = \phi_L$ corresponding to the switching between the orbital modes. The inset shows a typical dependence of the critical magnetic fields $H_L(T)$ for the orbital mode L . The numbers near the curves denote the corresponding values of vorticity L .

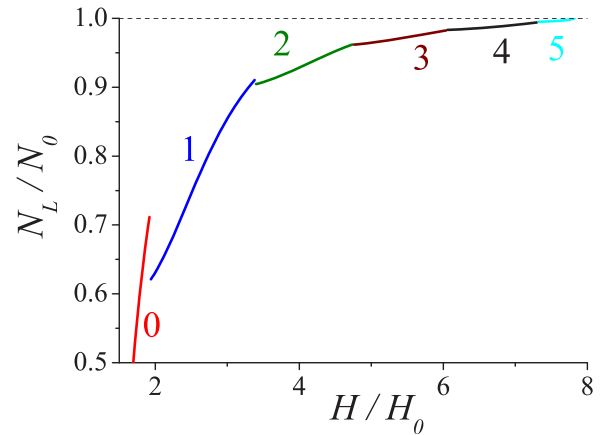


FIG. 4. The normalized LDOS N/N_0 at the disk edge versus the external magnetic field H (N_0 is the electronic density of states at the Fermi level) at $T = T_c(H) - 0.01T_{cs}$. Here we choose $R = 4\xi_0$, $g = 0.18$ and denote the corresponding values of vorticity L by numbers near the curves.

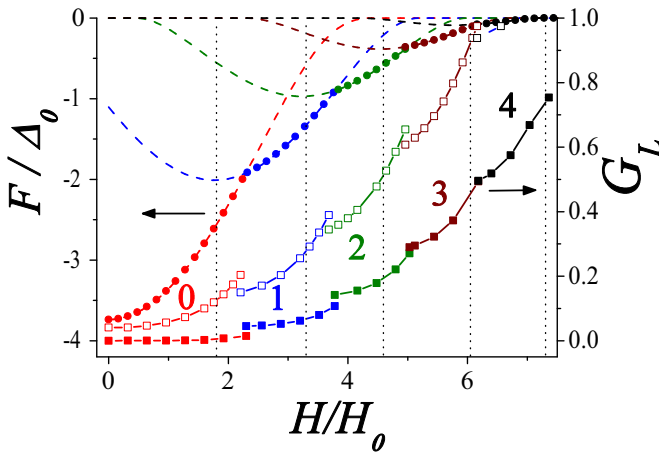


FIG. 5. The dependence of the free energy $F(\phi)$ (15) (symbol \bullet) and the normalized zero bias conductance (ZBC) $G_L(0, R, \phi)$ (16) at the disk edge for the temperatures $T = 0.1T_{cs}$ (symbol \blacksquare) and $T = 0.2T_{cs}$ (symbol \square) on the magnetic flux $\phi = H/H_0$ across the SC disk of the radius $R = 4\xi_0$. The dashed lines show the dependence $F_L(\phi)$ for fixed vorticity $L = 0-4$. The numbers near the curves denote the corresponding values of vorticity L . Vertical dotted lines $H/H_0 = \phi_L$ correspond to the switching of the orbital modes in the critical temperature T_c , shown in Fig. 2 ($F_0 = \pi \hbar D N_0 w \Delta_0$).

B. An arbitrary magnetic field: $0 < H < H_{c2}$

As a next step, we analyze the conductance behavior as a function of magnetic field and temperature at arbitrary magnetic fields, $0 < H < H_{c2}$. The Usadel equations (3)–(6) have been solved numerically for different vorticities, which allowed us to calculate and compare the values of the free energy.

Figure 5 shows the magnetic field dependence of the free energy F (15) and the zero bias conductance $G_L(0, R, \phi)$ (16) at the Fermi level for a small disk radius $R = 4\xi_0$ and two temperatures $T = 0.1T_{cs}$ and $T = 0.2T_{cs}$. All three curves illustrate the switching between the states with different

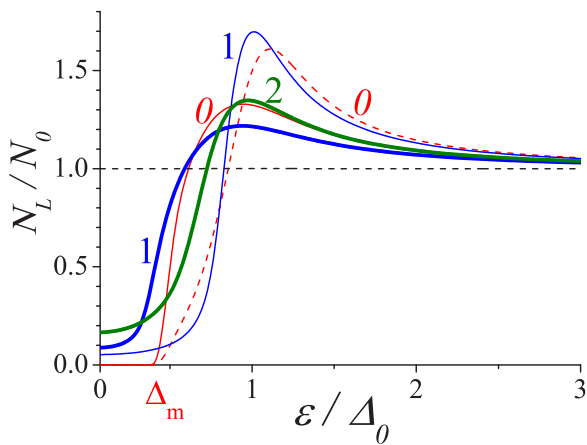


FIG. 6. Evolution of the spatially resolved LDOS $N(\varepsilon, r, \phi)$ in the disk center $r = 0$ (dashed lines) and the disk edge $r = R$ (solid lines) in the magnetic field: thin lines, $H/H_0 \simeq 2.24$; bold lines, $H/H_0 \simeq 3.84$ ($R = 4\xi_0$, $T = 0.1T_{cs}$). The numbers near the curves denote the corresponding values of vorticity L .

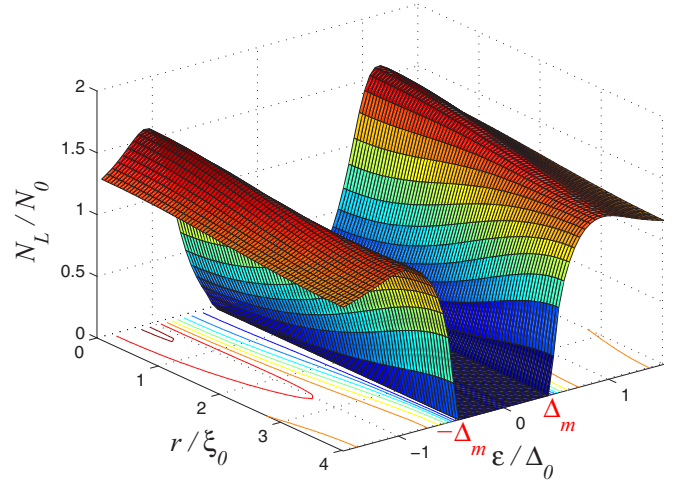


FIG. 7. Spatially resolved LDOS spectra $N_L(\varepsilon, r, H/H_0)$ of the Meissner state ($L = 0$) in the disk of the radius $R = 4\xi_0$ for the temperature $T = 0.1T_{cs}$ and the magnetic field $H = H_{s0} = 2.24H_0$ ($g = 0.18$).

vorticities $L = 0-4$, which are similar to the Little-Parks-like switching of the critical temperature $T_c(H)$, Fig. 2. Sequential entries of vortices produce a set of branches F_L with different vorticity L on the $F(H)$ and $dI/dV(H)$ curves. The transitions between different vortex states are accompanied by an abrupt change in the ZBC, which is attributed to the entry/exit of a vortex inside the disk while sweeping the magnetic field. We observe the Meissner state when the total vorticity $L = 0$ for $H \lesssim H_{s0} = 2.24H_0$, and a single-vortex state $L = 1$ in the field range $H_{s0} \lesssim H \lesssim H_{s1} = 3.84H_0$. In the Meissner state the ZBC is suppressed and spatially homogeneous: the ZBC value at the disk edge is slightly higher than ZBC value in the center. In the increasing magnetic field the gap in the tunneling spectra gradually fills with the quasiparticle states. This effect is more pronounced near the disk edge where the screening superconducting currents have higher density. The smooth evolution of ZBC continues till $H/H_0 \simeq 2.24$, where it is interrupted by a vortex entry. At higher fields $H > H_{s1}$ the multivortex states $L = 2-4$ become energetically favorable. Note that the field values H_{sL} at which the jumps in vorticity ($L \rightarrow L + 1$) occur are always larger than the values $H_0 \phi_L$ found from the calculations of the critical temperature behavior.

Figure 5 illustrates an important point noted in the Introduction, i.e., the temperature crossover between different regimes in the behavior of the conductance at the disk edge vs magnetic field. Indeed, one can clearly see that the change in temperature from $0.1T_{cs}$ to $0.2T_{cs}$ is accompanied by the change of the direction of jumps in the dependence of zero bias conductance vs magnetic field. The upward jumps in conductance for the lower temperature, $T < T^*(R)$, can be associated with the core-dominated regime $e^{-E_g/T} < e^{-R/d_L}$, see Fig. 1, when the conductance increases with the increase in the number of vortices trapped in the center of the sample and therefore in the parameter d_L . The downward jumps in conductance at higher temperatures, $T > T^*(R)$, are caused by the increase in the (soft) spectral gap value E_g at the sample

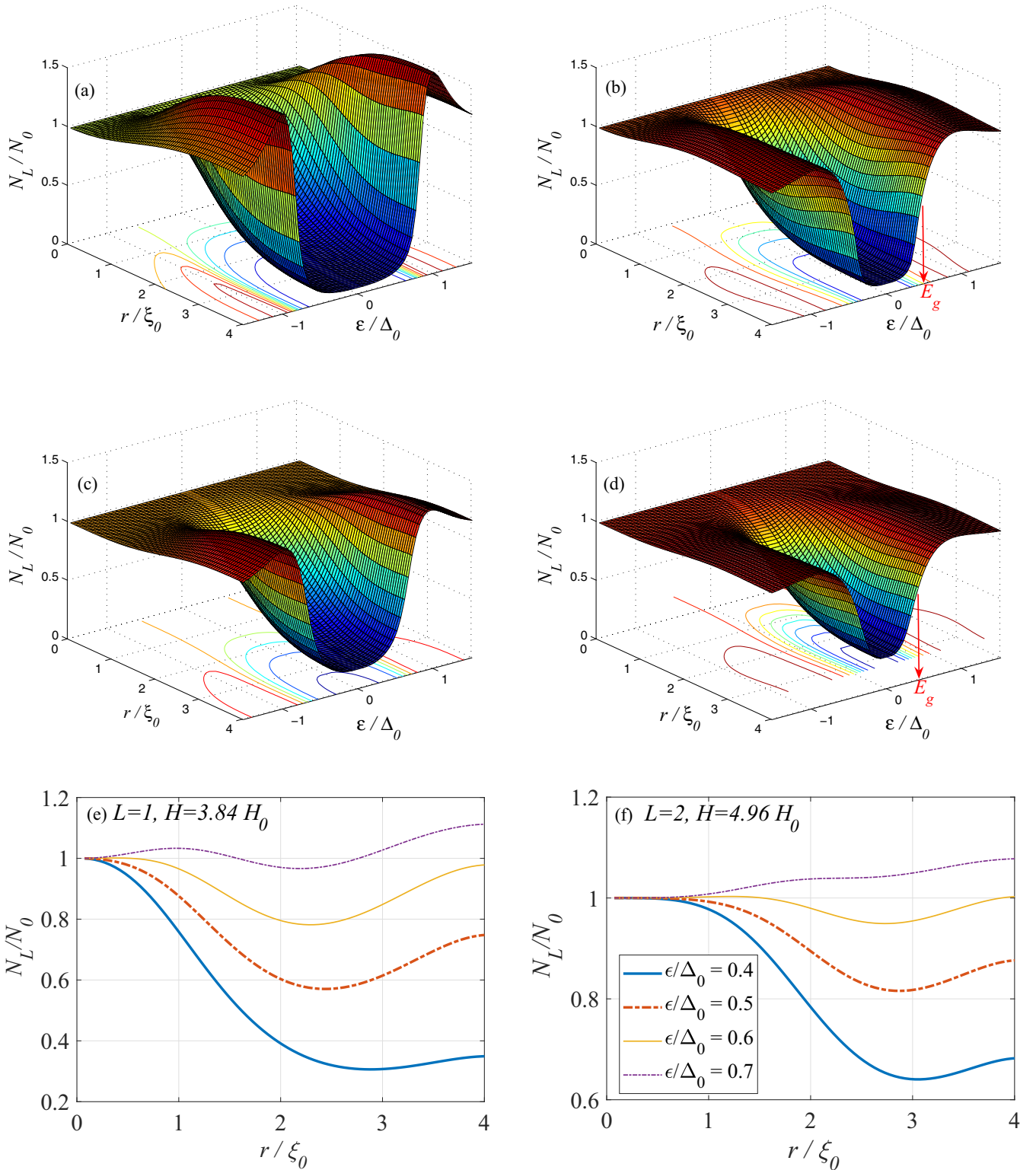


FIG. 8. Evolution of the LDOS $N_L(\epsilon, r, H/H_0)$ as a function of the energy ϵ and the distance from the vortex core r in the SC disk of the radius $R = 4\xi_0$ for the temperature $T = 0.1T_{cs}$ and different values of the magnetic field H : (a) $L = 1, H = H_{s0} \simeq 2.24H_0$; (b) $L = 1, H = H_{s1} \simeq 3.84H_0$; (c) $L = 2, H = H_{s1} \simeq 3.84H_0$; (d) $L = 2, H = H_{s2} \simeq 4.96H_0$. Panels (e) and (f) show the cross sections of (b) and (d), respectively, at energies $\epsilon/\Delta_0 = 0.4, 0.5, 0.6$, and 0.7 from bottom to top.

edge as the vortex enters, which should result in the suppression of the subgap conductance $G_L \sim e^{-E_g/T}$. The change in vorticity $L \rightarrow L + 1$ in this case results in the decrease of the screening current density and the corresponding enhancement

of superconductivity at the edge of the disk. Assuming the crossover temperature $T^*(R)$ to be in the interval $0.1T_{cs} < T^*(R) < 0.2T_{cs}$ and taking $R = 4\xi_0$ one can estimate the value $E_g \sim 0.8\Delta_0$, which is in good agreement with the behavior

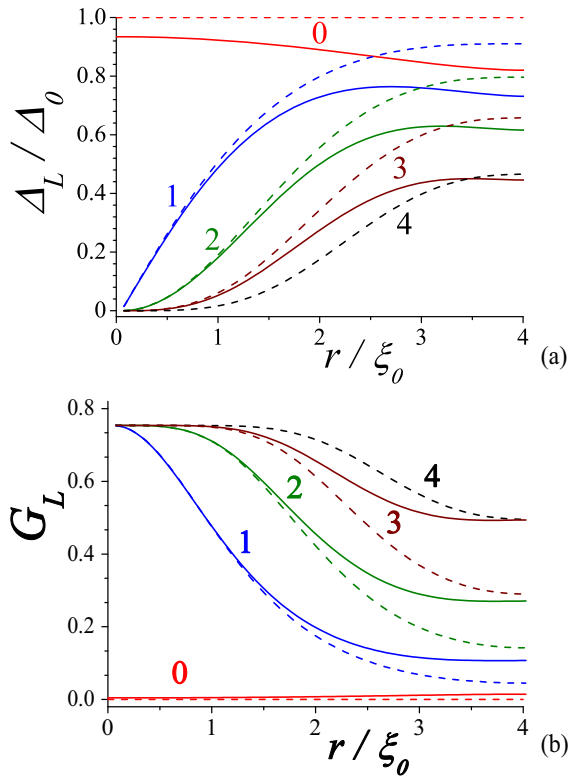


FIG. 9. The radial dependence of the SC order parameter Δ_L (a) and ZBC $G_L(0, R, \phi)$ (b) for minimal (dashed line) and maximal (solid line) allowed values of the magnetic field H for the orbital mode L : $L = 0 - H/H_0 = 0, 2.24$; $L = 1 - H/H_0 = 2.24, 3.84$; $L = 2 - H/H_0 = 3.84, 4.96$; $L = 3 - H/H_0 = 4.96, 6.08$; $L = 4 - H/H_0 = 6.08$ ($R = 4\xi_0, T = 0.1T_c$). The numbers near the curves denote the corresponding values of vorticity L .

of the energy dependence of the local density of states in Figs. 6 and 8. Indeed, each vorticity jump increases both the zero-energy LDOS value and the soft minigap at the edge E_g , corresponding to the maximal slope of the energy dependence of the LDOS and roughly giving $E_g \lesssim 0.8\Delta_0$, Fig. 6. The LDOS spatial growth $N_L(\varepsilon, r, \phi)$ near the disk edge ($r \lesssim R$) is observed for energies $\varepsilon > E_g \simeq 0.4\Delta_0$ if the magnetic field is equal to the maximal value H_{sL} for L orbital mode [see Figs. 8(b), 8(d)–8(f)]. At the same time, the vortex core size depends slightly on the applied magnetic field for a fixed vorticity L , $H_{sL-1} < H < H_{sL}$ [cf. Figs. 8(a), 8(c) and 8(b), 8(d)]. It gives evidence that the LDOS increase at the edge shown is produced by screening currents due to the size effect in a small disk, rather than by the expansion of the vortex core. Figures 7 and 8 also illustrate the switching between the states with hard and soft gaps with the magnetic field increase. In the Meissner state ($H < H_{s0}$), Fig. 7, the hard minigap Δ_m in the spectrum survives [$N(\varepsilon < \Delta_m, r, H/H_0) = 0$] until the first vortex entry, Fig. 8(a). The density of states in the center of the disk $N(\varepsilon, 0, \phi)$ is equal to the electronic density of states at the Fermi level N_0 for any vortex state $L \geq 1$, indicating a full suppression of the spectral gap in the disk center due to the vortex entry. At the same time, at the edge of the disk

the superconductivity survives though the gap becomes soft, $0 < N(0, R, \phi) < N_0$.

Figure 9 presents the radial distributions of the SC order parameter $\Delta_L(r)$ and the ZBC dI/dV at $T = 0.1T_c$ for different values of the magnetic field H corresponding to the switching between the states with different vorticity L . The profiles of ZBC in multiquantum vortices $L > 1$ reveal a plateau near the vortex center, which can be considered as a hallmark of the multiquantum vortex formation in dirty mesoscopic superconductors [21,22,41].

The electronic properties of the vortex states look to be rather different if the radius of the disk R is much larger than the coherence length ξ_0 . In this case the core of a multiquantum vortex does not extend to the edge of the disk, and quasiparticles in the vortex core remain well localized near the disk center. Clearly, in this case the temperature crossover between the core-dominated and edge-dominated regimes accompanied by the change in the direction of the jumps in the local ZBC at the sample edge becomes much more difficult to observe due to the exponentially small values of the factors $\exp(-R/d_L)$ and $\exp(-E_g/T)$ near the crossover.

V. CONCLUSIONS

To sum up, we have analyzed the behavior of the LDOS $N(\varepsilon, r, H)$ and conductance on an external magnetic field H in a mesoscopic superconducting disk on the basis of Usadel equations. We have demonstrated that transitions between the superconducting states with different vorticities provoke abrupt changes (jumps) in the local zero bias conductance dI/dV at the edge of the disk. These jumps of the ZBC are attributed to the entry/exit of vortices while sweeping the magnetic field. The transitions between different vortex states can be accompanied by both the decrease and increase in the ZBC while sweeping the magnetic field up. The direction of jumps in ZBC attributed to the vortex entry depends on the disk radius R and the temperature T and is determined by two opposite-in-sign contributions to conductance: (i) the entrance of a vortex into the disk is accompanied by the reduction of the supercurrents flowing along the sample edge and, thus, improves superconductivity at the edge; (ii) the entrance of a vortex increases the number of subgap quasiparticle states in the multiquantum vortex core, which provides an additional contribution to the conductance because of the quasiparticle tunneling between the vortex core and the sample edge. To the best of our knowledge, the systematic experimental analysis of the direction of the ZBC jumps has not been done yet. However, these measurements can provide additional information about the soft gap value governing not only the contribution to the tunneling transport, but also the one to the thermal relaxation mechanisms (see, e.g., [46,52]) and also about the classical-to-quantum interplay in quasiparticle tunneling in mesoscopic superconducting samples. These results are directly related to the quantitative characterization of the quasiparticle traps appearing in the Meissner and vortex states of superconductors (see, e.g., [46–52]), especially in the different types of single-electron sources based on hybrid superconducting junctions and working far from equilibrium [46,52,63–65].

ACKNOWLEDGMENTS

This work was supported, in part, by the Russian Foundation for Basic Research under Grant No. 17-52-12044 and the Foundation for the Advancement to Theoretical Physics and Mathematics “BASIS” Grant No. 17-11-109. In the part concerning the numerical calculations of the local density of states, the work was supported by Russian Science Foundation (Grant No. 17-12-01383). I.M.K. acknowledges the support of the German Research Foundation (DFG) Grant No. KH 425/1-1. A.S.M. and A.V.S. appreciate warm hospitality of the Max-Planck Institute for the Physics of Complex Systems, Dresden, Germany, extended to them during their visits when this work was done.

APPENDIX: SOLUTION OF EQ. (7)
VIA KUMMER'S FUNCTION

Substituting the expression of the order parameter $\Delta_L(r) = \theta_L(r)(\omega_n + \Omega_L)$, Eq. (9), into Eq. (7) and rewriting the latter in terms of the renormalized flux $\phi_r = \pi r^2 H / \Phi_0$,

$$\frac{d}{d\phi_r} \left(\phi_r \frac{d\theta_L}{d\phi_r} \right) - \frac{(L - \phi_r)^2}{4\phi_r} \theta_L + \frac{\Phi_0 \Omega_L}{2\pi \hbar D H} \theta_L = 0, \quad (\text{A1})$$

one can easily obtain the equation for the function $W(\phi_r)$ defined as

$$\theta_L(r) = e^{-\phi_r/2} \phi_r^{|L|/2} W(\phi_r), \quad (\text{A2})$$

$$\phi_r \frac{d^2 W}{d\phi_r^2} + (b_L - \phi_r) \frac{dW}{d\phi_r} - a_L W = 0, \quad (\text{A3})$$

with the parameters a_L and b_L given by

$$a_L = \frac{1}{2} \left(|L| - L + 1 - \frac{\Phi_0 \Omega_L}{\pi \hbar D H} \right), \quad b_L = |L| + 1. \quad (\text{A4})$$

The solution of Eq. (A3) in the region $r \leq R$ is a confluent hypergeometric function of the first kind (Kummer's function), $W = K(a_L, b_L, \phi_r)$, which after substitution into the expression (A2) for $\theta_L(r)$ gives the result (10) from the main text.

-
- [1] H. J. Fink and A. G. Presson, Superheating of the Meissner state and the giant vortex state of a cylinder of finite extent, *Phys. Rev.* **168**, 399 (1968).
- [2] A. I. Buzdin and J. P. Brison, Vortex structures in small superconducting disks, *Phys. Lett. A* **196**, 267 (1994).
- [3] V. V. Moshchalkov, L. Gielen, C. Strunk, R. Jonckheere, X. Qiu, C. Van Haesendonck, and Y. Bruynseraede, Effect of sample topology on the critical fields of mesoscopic superconductors, *Nature (London, U.K.)* **373**, 319 (1995).
- [4] A. K. Geim, I. V. Grigorieva, S. V. Dubonos, J. G. S. Lok, J. C. Maan, A. E. Filippov, and F. M. Peeters, Phase transitions in individual sub-micrometre superconductors, *Nature (London, U.K.)* **390**, 259 (1997).
- [5] O. Buisson, P. Gandit, R. Rammal, Y. Y. Wang, and B. Pannetier, Magnetization oscillations of a superconducting disk, *Phys. Lett. A* **150**, 36 (1990).
- [6] A. K. Geim, S. V. Dubonos, J. J. Palacios, I. V. Grigorieva, M. Henini, and J. J. Schermer, Fine Structure in Magnetization of Individual Fluxoid States, *Phys. Rev. Lett.* **85**, 1528 (2000).
- [7] V. A. Schweigert, F. M. Peeters, and P. S. Deo, Vortex Phase Diagram for Mesoscopic Superconducting Disks, *Phys. Rev. Lett.* **81**, 2783 (1998).
- [8] J. J. Palacios, Vortex matter in superconducting mesoscopic disks: Structure, magnetization, and phase transitions, *Phys. Rev. B* **58**, R5948 (1998).
- [9] V. Bruyndoncx, J. G. Rodrigo, T. Puig, L. Van Look, V. V. Moshchalkov, and R. Jonckheere, Giant vortex state in perforated aluminum microsquares, *Phys. Rev. B* **60**, 4285 (1999).
- [10] H. T. Jadallah, J. Rubinstein, and P. Sternberg, Phase Transition Curves for Mesoscopic Superconducting Samples, *Phys. Rev. Lett.* **82**, 2935 (1999).
- [11] L. F. Chibotaru, A. Ceulemans, V. Bruyndoncx, and V. V. Moshchalkov, Symmetry-induced formation of antivortices in mesoscopic superconductors, *Nature (London, U.K.)* **408**, 833 (2000).
- [12] A. S. Mel'nikov and V. M. Vinokur, Mesoscopic superconductor as a ballistic quantum switch, *Nature (London, U.K.)* **415**, 60 (2002).
- [13] A. S. Mel'nikov, I. M. Nefedov, D. A. Ryzhov, I. A. Shereshevskii, V. M. Vinokur, and P. P. Vysheslavtsev, Vortex states and magnetization curve of square mesoscopic superconductors, *Phys. Rev. B* **65**, 140503(R) (2002).
- [14] R. Geurts, M. V. Milosevic, and F. M. Peeters, Symmetric and Asymmetric Vortex-Antivortex Molecules in a Four-fold Superconducting Geometry, *Phys. Rev. Lett.* **97**, 137002 (2006).
- [15] M. Amundsen, J. A. Ouassou, and J. Linder, Field-Free Nucleation of Antivortices and Giant Vortices in Nonsuperconducting Materials, *Phys. Rev. Lett.* **120**, 207001 (2018).
- [16] M. Morelle, J. Bekaert, and V. V. Moshchalkov, Influence of the sample geometry on the vortex matter in superconducting microstructures, *Phys. Rev. B* **70**, 094503 (2004).
- [17] T. Nishio, Q. Chen, W. Gillijns, K. De Keyser, K. Vervaeke, and V. V. Moshchalkov, Scanning Hall probe microscopy of vortex patterns in a superconducting microsquare, *Phys. Rev. B* **77**, 012502 (2008).
- [18] H. J. Zhao, V. R. Misko, F. M. Peeters, V. Oboznov, S. V. Dubonos, and I. V. Grigorieva, Vortex states in mesoscopic superconducting squares: Formation of vortex shells, *Phys. Rev. B* **78**, 104517 (2008).
- [19] N. Kokubo, S. Okayasu, A. Kanda, and B. Shinozaki, Scanning SQUID microscope study of vortex polygons and shells in weak-pinning disks of an amorphous superconducting film, *Phys. Rev. B* **82**, 014501 (2010).
- [20] A. Kanda, B. J. Baelus, F. M. Peeters, K. Kadowaki, and Y. Ootuka, Experimental Evidence for Giant Vortex States in a

- Mesoscopic Superconducting Disk, *Phys. Rev. Lett.* **93**, 257002 (2004).
- [21] T. Cren, D. Fokin, F. Debontridder, V. Dubost, and D. Roditchev, Ultimate Vortex Confinement Studied by Scanning Tunneling Spectroscopy, *Phys. Rev. Lett.* **102**, 127005 (2009).
- [22] T. Cren, L. Serrier-Garcia, F. Debontridder, and D. Roditchev, Vortex Fusion and Giant Vortex States in Confined Superconducting Condensates, *Phys. Rev. Lett.* **107**, 097202 (2011).
- [23] T. Nishio, T. An, A. Nomura, K. Miyachi, T. Eguchi, H. Sakata, S. Lin, N. Hayashi, N. Nakai, M. Machida, and Y. Hasegawa, Superconducting Pb Island Nanostructures Studied by Scanning Tunneling Microscopy and Spectroscopy, *Phys. Rev. Lett.* **101**, 167001 (2008).
- [24] M. Timmermans, L. Serrier-Garcia, M. Perini, J. Van de Vondel, and V. V. Moshchalkov, Direct observation of condensate and vortex confinement in nanostructured superconductors, *Phys. Rev. B* **93**, 054514 (2016).
- [25] H. F. Hess, R. B. Robinson, R. C. Dynes, J. M. Wallis, Jr., and J. V. Waszczak, Scanning-Tunneling-Microscope Observation of the Abrikosov Flux Lattice and the Density of States near and inside a Fluxoid, *Phys. Rev. Lett.* **62**, 214 (1989).
- [26] H. F. Hess, R. B. Robinson, and J. V. Waszczak, Vortex-Core Structure Observed with a Scanning Tunneling Microscope, *Phys. Rev. Lett.* **64**, 2711 (1990).
- [27] F. Gygi and M. Schluter, Self-consistent electronic structure of a vortex line in a type-II superconductor, *Phys. Rev. B* **43**, 7609 (1991).
- [28] Y. Tanaka, A. Hasegawa, and H. Takayanagi, Energy spectrum of the quasiparticle in a quantum dot formed by a superconducting pair potential under a magnetic field, *Solid State Commun.* **85**, 321 (1993).
- [29] Y. Tanaka, S. Kashiwaya, and H. Takayanagi, Theory of superconducting quantum dot under magnetic field, *Jpn. J. Appl. Phys.* **34**, 4566 (1995).
- [30] D. Rainer, J. A. Sauls, and D. Waxman, Current carried by bound states of a superconducting vortex, *Phys. Rev. B* **54**, 10094 (1996).
- [31] S. M. M. Virtanen and M. M. Salomaa, Multiquantum vortices in superconductors: Electronic and scanning tunneling microscopy spectra, *Phys. Rev. B* **60**, 14581 (1999).
- [32] M. Eschrig, D. Rainer, and J. A. Sauls, Vortex core structure and dynamics in layered superconductors, in *Vortices in Unconventional Superconductors and Superfluids* edited by R. P. Huebener, N. Schopohl, and G. E. Volovik (Springer Verlag, Berlin, 2002), p. 175.
- [33] K. Tanaka, I. Robel, and B. Janko, Electronic structure of multiquantum giant vortex states in mesoscopic superconducting disks, *Proc. Natl. Acad. Sci. USA* **99**, 5233 (2002).
- [34] N. B. Kopnin, A. S. Mel'nikov, V. I. Pozdnyakova, D. A. Ryzhov, I. A. Shereshevskii, and V. M. Vinokur, Giant Oscillations of Energy Levels in Mesoscopic Superconductors, *Phys. Rev. Lett.* **95**, 197002 (2005).
- [35] A. S. Mel'nikov, D. A. Ryzhov, and M. A. Silaev, Electronic structure and heat transport of multivortex configurations in mesoscopic superconductors, *Phys. Rev. B* **78**, 064513 (2008).
- [36] A. S. Mel'nikov, D. A. Ryzhov, and M. A. Silaev, Local density of states around single vortices and vortex pairs: Effect of boundaries and hybridization of vortex core states, *Phys. Rev. B* **79**, 134521 (2009).
- [37] L.-F. Zhang, L. Covaci, M. V. Milosevic, G. R. Berdiyrov, and F. M. Peeters, Unconventional Vortex States in Nanoscale Superconductors due to Shape-Induced Resonances in the Inhomogeneous Cooper-Pair Condensate, *Phys. Rev. Lett.* **109**, 107001 (2012).
- [38] G. E. Volovik, Vortex motion in Fermi superfluids and Callan-Harvey effect, *Pis'ma Zh. Eksp. Teor. Fiz.* **57**, 233 (1993) [*JETP Lett.* **57**, 244 (1993)].
- [39] R. Watts-Tobin, L. Kramer, and W. Pesch, Density of states, entropy, and specific heat for dirty type-II superconductors at arbitrary temperature, *J. Low Temp. Phys.* **17**, 71 (1974).
- [40] A. A. Golubov and U. Hartmann, Electronic Structure of the Abrikosov Vortex Core in Arbitrary Magnetic Fields, *Phys. Rev. Lett.* **72**, 3602 (1994).
- [41] M. A. Silaev and V. A. Silaeva, Self-consistent electronic structure of multiquantum vortices in superconductors at $T \ll T_c$, *J. Phys.: Condens. Matter* **25**, 225702 (2013).
- [42] N. B. Kopnin, I. M. Khaymovich, and A. S. Mel'nikov, Predicted Multiple Cores of a Magnetic Vortex Threading a Two-Dimensional Metal Proximity Coupled to a Superconductor, *Phys. Rev. Lett.* **110**, 027003 (2013).
- [43] N. B. Kopnin, I. M. Khaymovich, and A. S. Mel'nikov, Vortex matter in low-dimensional systems with proximity-induced superconductivity, *J. Exp. Theor. Phys.* **117**, 418 (2013).
- [44] H. Q. Nguyen, T. Aref, V. J. Kauppila, M. Meschke, C. B. Winkelmann, H. Courtois, and J. P. Pekola Trapping hot quasiparticles in a high-power superconducting electronic cooler, *New J. Phys.* **15**, 085013 (2013).
- [45] J. N. Ullom, P. A. Fisher, and M. Nahum, Magnetic field dependence of quasiparticle losses in a superconductor, *Appl. Phys. Lett.* **73**, 2494 (1998).
- [46] M. Taupin, I. M. Khaymovich, M. Meschke, A. S. Mel'nikov, and J. P. Pekola, Tunable quasiparticle trapping in Meissner and vortex states of mesoscopic superconductors, *Nat. Commun.* **7**, 10977 (2016).
- [47] J. T. Peltonen, J. T. Muhonen, M. Meschke, N. B. Kopnin, and J. P. Pekola, Magnetic-field-induced stabilization of nonequilibrium superconductivity in a normal-metal/insulator/superconductor junction, *Phys. Rev. B* **84**, 220502(R) (2011).
- [48] I. Nsanzineza and B. L. T. Plourde, Trapping a Single Vortex and Reducing Quasiparticles in a Superconducting Resonator, *Phys. Rev. Lett.* **113**, 117002 (2014).
- [49] C. Wang, Y. Y. Gao, I. M. Pop, U. Vool, C. Axline, T. Brecht, R. W. Heeres, L. Frunzio, M. H. Devoret, G. Catelani, L. I. Glazman and R. J. Schoelkopf, Measurement and control of quasiparticle dynamics in a superconducting qubit, *Nat. Commun.* **5**, 5836 (2014).
- [50] U. Vool, I. M. Pop, K. Sliwa, B. Abdo, C. Wang, T. Brecht, Y. Y. Gao, S. Shankar, M. Hatridge, G. Catelani, M. Mirrahimi, L. Frunzio, R. J. Schoelkopf, L. I. Glazman, and M. H. Devoret, Non-Poissonian Quantum Jumps of a Fluxonium Qubit due to Quasiparticle Excitations, *Phys. Rev. Lett.* **113**, 247001 (2014).
- [51] D. J. van Woerkom, A. Geresdi, and L. P. Kouwenhoven, One minute parity lifetime of a NbTiN Cooper-pair transistor, *Nat. Phys.* **11**, 547 (2015).
- [52] S. Nakamura, Y. A. Pashkin, M. Taupin, V. F. Maisi, I. M. Khaymovich, A. S. Mel'nikov, J. T. Peltonen, J. P. Pekola, Y.

- Okazaki, S. Kashiwaya, S. Kawabata, A. S. Vasenko, J.-S. Tsai, and N.-H. Kaneko, Interplay of the Inverse Proximity Effect and Magnetic Field in Out-of-Equilibrium Single-Electron Devices, *Phys. Rev. Appl.* **7**, 054021 (2017).
- [53] C. Caroli, P. G. de Gennes, and J. Matricon, Bound Fermion states on a vortex line in a type II superconductor, *Phys. Lett.* **9**, 307 (1964).
- [54] S. Skalski, O. Betbeder-Matibet, and P. R. Weiss, Properties of superconducting alloys containing paramagnetic impurities, *Phys. Rev.* **136**, A1500 (1964).
- [55] K. Maki and P. Fulde, Equivalence of different pair-breaking mechanisms in superconductors, *Phys. Rev.* **140**, A1586 (1965).
- [56] P. Fulde, Tunneling density of states for a superconductor carrying a current, *Phys. Rev.* **137**, A783 (1965).
- [57] A. Anthore, H. Pothier, and D. Esteve, Density of States in a Superconductor Carrying a Supercurrent, *Phys. Rev. Lett.* **90**, 127001 (2003).
- [58] I. Guillamon, H. Suderow, S. Vieira, A. Fernandez-Pacheco, J. Sese, R. Cordoba, J. M. De Teresa, and M. R. Ibarra, Superconducting density of states at the border of an amorphous thin film grown by focused-ion-beam, *J. Phys.: Conf. Ser.* **150**, 052064 (2009).
- [59] K. D. Usadel, Generalized Diffusion Equation for Superconducting Alloys, *Phys. Rev. Lett.* **25**, 507 (1970).
- [60] M. Abramowitz and I. A. Stegun, *Handbook of Mathematical Functions* (Dover Publications, New York, 1972).
- [61] W. A. Little and R. D. Parks, Observation of Quantum Periodicity in the Transition Temperature of a Superconducting Cylinder, *Phys. Rev. Lett.* **9**, 9 (1962).
- [62] R. D. Parks and W. A. Little, Fluxoid quantization in a multiply-connected superconductor, *Phys. Rev.* **133**, A97 (1964).
- [63] I. M. Khaymovich, V. F. Maisi, J. P. Pekola, and A. S. Mel'nikov, Charge-vortex interplay in a superconducting Coulomb-blockaded island, *Phys. Rev. B* **92**, 020501(R) (2015).
- [64] I. M. Khaymovich and D. M. Basko, Recovery of SINIS turnstile accuracy in a strongly nonequilibrium regime, *Phys. Rev. B* **94**, 165158 (2016).
- [65] D. M. T. van Zanten, D. M. Basko, I. M. Khaymovich, J. P. Pekola, H. Courtois, and C. B. Winkelmann, Single Quantum Level Electron Turnstile, *Phys. Rev. Lett.* **116**, 166801 (2016).